

Supporting Information

**High toughness supramolecular double network hydrogel electrolytes
for artificial flexible and low-temperature tolerant sensor**

Guoqi Chen,^a Jianren Huang,^{b, c} Jianfeng Gu,^a Shuijiao Peng,^a Xiaotong Xiang,^a Kai
Chen,^a Xiaoxiang Yang,^b Lunhui Guan,^c Xiancai Jiang^{*a, d}, Linxi Hou^{*a}

a. School of Chemical Engineering, Fuzhou University, Fuzhou 350108, China
E-mail: jiangxc@fzu.edu.cn; lxhou@fzu.edu.cn

b. School of Mechanical Engineering and Automation, Fuzhou University, Fuzhou
350108, China

c. CAS Key Laboratory of Design and Assembly of Functional Nanostructures, Fujian
Key Laboratory of Nanomaterials, Fujian Institute of Research on the Structure of
Matter, Chinese Academy of Sciences, Fuzhou 350002, China

d. State Key Laboratory of Polymer Materials Engineering, Sichuan University,
Chengdu 610065, China

Experimental

1. Materials

PVA (degree of polymerization is 1700, degree of alcoholysis is 99%) and AM were provided by Zhiyuan Chemical Co. (Tianjin, China). N, N'-methylenebisacrylamide (MBA) was acquired from Damao Chemical Reagent (Tianjin, China). 2-hydroxy-4-(2-hydroxyethoxy)-2-methylpropiophenone (Irgacure 2959) was procured from BASF (China). Distilled water was used throughout the experiment.

2. Fabrication of PVA/PAM/NaCl DN hydrogel electrolytes

Firstly, 0.2 g PVA and a certain amount of NaCl (as shown in Table S3) was added into 7 mL distilled water. PVA was stirred and heated until completely dissolving in a water bath at 90 °C. Then, 2.1 g AM, 0.0662 g Irgacure 2959 and 1.36 mg MBA were added into PVA/NaCl solution and stirred until all components were dissolved. Finally, the resulting solution was injected into different molds, and placed it under UV light ($\lambda = 365$ nm wavelength, intensity of 8 W) for 1 h to cause the gelation.

3. Optical characterization

The FTIR spectra of PVA/PAM/NaCl hydrogel electrolytes were noted at a FTIR infrared spectrometer (Nicolet iS50, Thermo Fisher Scientific, USA) in the wavenumber range of 4000-500 cm^{-1} and a resolution of 4 cm^{-1} . The crystalline properties of PVA/PAM/NaCl hydrogel electrolytes were characterized by X-ray diffractometer (DY5261/Xpert3, CEM, America) with the Cu $K\alpha$ radiation (40 kV, 40 mA, $\lambda = 1.542$ nm) at room temperature. The measurements were performed at the 2 theta range of 5-65°. Morphological details of PVA/PAM/NaCl hydrogel electrolytes were obtained by SEM instrument (FEI Nova Nano-SEM 230, America) with the primary electron energy of 10.0 kV. PVA/PAM/NaCl hydrogel electrolyte samples were firstly brittle fractured in liquid nitrogen and freeze dried, then the cross sections were vacuum coated with gold. Their UV-visible light barrier properties were performed by a Thermo Fisher GENESYS 10S UV-Vis, and measured at the UV wavelength from 400 to 700 nm.

4. Mechanical characterization

Stretching and compressing capability of hydrogels were measured by an electrical universal material testing machine (MTS CMT4104). The hydrogel samples were cut into dumbbell-shape which was 75 mm long, 4 mm wide and 2 mm thick. The integral of the area under the tensile stress-strain curve gave the fracture energy of the hydrogels. Hydrogels were stretched in the speed of 100 mm/min. The testing temperature is 20 °C and the humidity is 54%. The fracture energy (U_i) was calculated according to the following equation:

$$U_i = \int \tau d\varepsilon \quad (1)$$

where τ was stress, and ε was strain.

For the loading-unloading measurement, the hysteresis energy (ΔU_i) and the energy loss coefficient (η) was calculated as follows:

$$\Delta U_i = \int_{loading} \tau d\varepsilon - \int_{unloading} \tau d\varepsilon \quad (2)$$

$$\eta = \Delta U_i / U_i \quad (3)$$

The energy loss coefficient (η) was calculated as tensile loading-unloading test.

The hydrogels were made into a cylinder with a height of 15 mm and a diameter of 22 mm. Integral the area of compression curve gave the dissipation energy of the hydrogels. Hydrogels were compressed in the speed of 5 mm/min at the temperature of 20 °C and humidity of 54%. For the compression-recovery measurement, the hysteresis energy (ΔU_i) was calculated as follows:

$$\Delta U_i = \int_{compression} \tau d\varepsilon - \int_{recover} \tau d\varepsilon \quad (4)$$

5. Electrical characterization

The ionic conductivity of the hydrogels was measured by the impedance spectrum in a frequency range of 1 to 1×10^6 Hz. Hydrogels were prepared into a sheet with a cross-sectional area (A) of 1 cm² and a thickness (d) of 2 mm. The hydrogel sheets were sandwiched between two pieces of foamed nickel mesh. The resistance (R) was the intercept through the horizontal axis in the EIS diagram. The conductivity (σ) was calculated by the following formula:

$$\sigma = \frac{d}{AR} \quad (5)$$

The hydrogels were deployed as sensitive material (dumbbell-shape which was 75 mm long, 4 mm wide and 2 mm thick) to fabricate strain sensors using the two-electrode configuration. Two copper tapes were adhered to the hydrogels at a distance of 40 mm using copper tape to ensure a good ohmic contact between the parts. To apply desired strains to the sensor for the electrochemical test, the two ends of the samples were fixed on a stretching machine (AG-X plus, Shimadzu, Japan). Both the electrical resistance and mechanical strain of the sensor during the testing were measured simultaneously and recorded continuously by a digital Multimeter (Keithley 2450) through the Lab VIEW software. The experimental setup of self-strain sensing is shown in Fig. S15.

6. Thermal characterization

The thermal property of PVA/PAM/NaCl DN hydrogels was measured by the NETZSCH DSC214. 5-10 mg hydrogel sample was placed in the aluminum pan and then sealed with a pressing tool. An empty pan was used as a reference. All of the samples were equilibrated at -40 °C for 3 min, ramped at 1 °C/min to 60 °C under nitrogen atmosphere. METTLER TOLEDO DMA1 was used to measure dynamic thermo-mechanical property in the tensile mode and at a frequency of 1 Hz. All of the measurements were carried out between -40 °C and 60 °C at the heating rate of 3 °C/min in a nitrogen atmosphere. The hydrogels with the dimension of $4 \times 10 \times 0.1$ mm were subjected to sinusoidal deformation with a 10 μ m amplitude.

Table S1

Comparison of mechanical property and conductivity for PVA/PAM/NaCl and different component hydrogels.

Component	Stress (MPa)	Strain (%)	Conductivity (S/m)	Ref.
Allyl Cellulose	0.037	126	0.016	[1]
PANI/PSS	0.1	700	13	[2]
PAAm/PVA/MXene/EG	0.035	1000	0.017	[3]
PVA/HPC	1.3	950	3.4	[4]
PVA/PAM/NaCl	0.48	1072	6.23	This work

Table S2

Comparison of PVA/PAM/NaCl hydrogel electrolytes based strain sensors and previously reported hydrogel based sensors.

Materials	Strain (%)	Sensitivity	Conductivity (S/m)	Ref
MBAA/HEMA	100	1.8	0.24	[5]
PANI/UPy/ANI	300	3.4	14.2	[2]
PAAm/PVA/MXene/EG	335	44.85	0.045	[3]
PVA/PSBMA	50	1.5	0.0368	[6]
HPC/PVA	400	2	3.4	[4]
PANI/PAAm/HEMA	70	11	8.24	[7]
PVA/CNT	1000	1.5	N/A	[8]
PDA/PAM	1000	0.693	N/A	[9]
PAA/Fe ₃ O ₄	1400	20.2	0.26	[10]
PVA/PAM/NaCl	950	24.901	6.23	Our work

Table S3

The experimental ingredients and nomenclatures of PVA/PAM and PVA/PAM/NaCl hydrogel electrolytes.

Sample	PVA (g)	AM (g)	Irgacure 2959 (g)	MBA (mg)	Distilled water (g)	NaCl (g)
PVA/PAM	0.2	2.1	0.0662	1.36	7.0	/
PVA/PAM/NaCl-1	0.2	2.1	0.0662	1.36	7.0	0.35
PVA/PAM/NaCl-2	0.2	2.1	0.0662	1.36	7.0	0.70
PVA/PAM/NaCl-3	0.2	2.1	0.0662	1.36	7.0	1.05
PVA/PAM/NaCl-4	0.2	2.1	0.0662	1.36	7.0	1.40

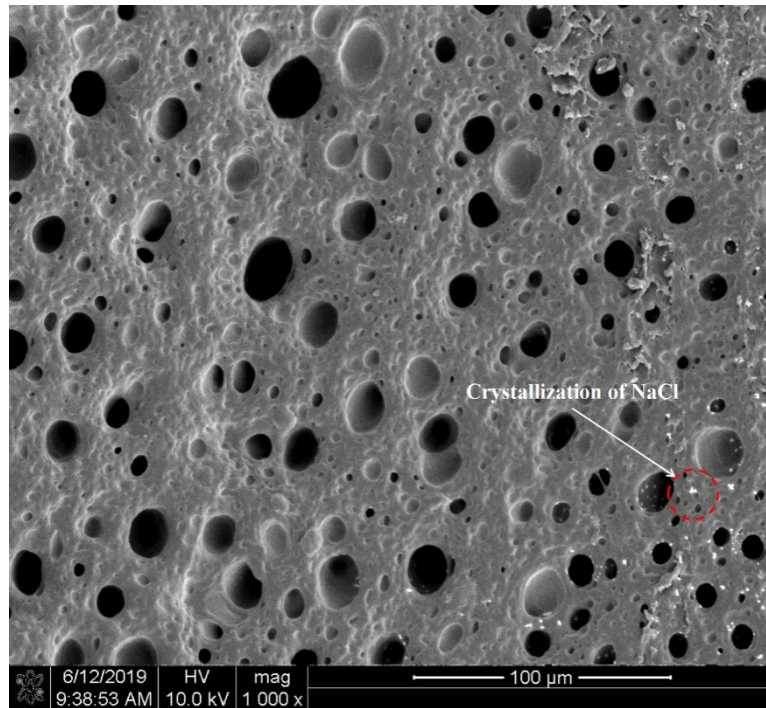


Figure S1. SEM image of PVA/PAM/NaCl DN hydrogel electrolyte with the NaCl crystals.

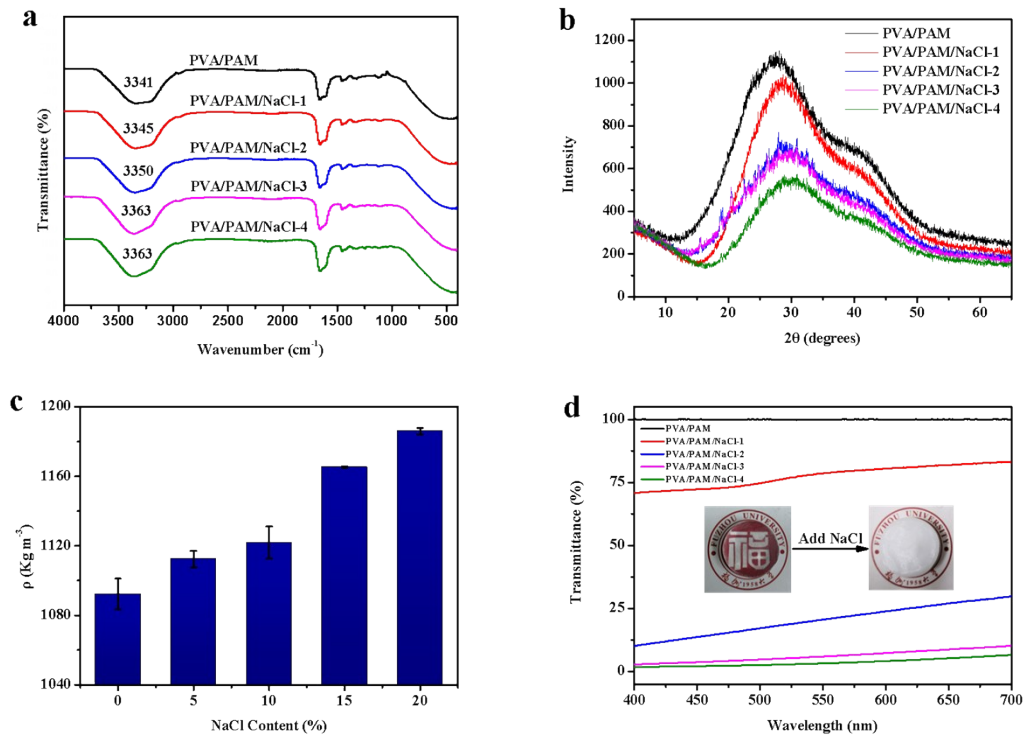


Figure S2. a) FTIR spectra, b) XRD patterns, c) Effect of NaCl content on density and d) UV transmittance curve of PVA/PAM DN hydrogel electrolytes and PVA/PAM/NaCl DN hydrogel electrolytes.

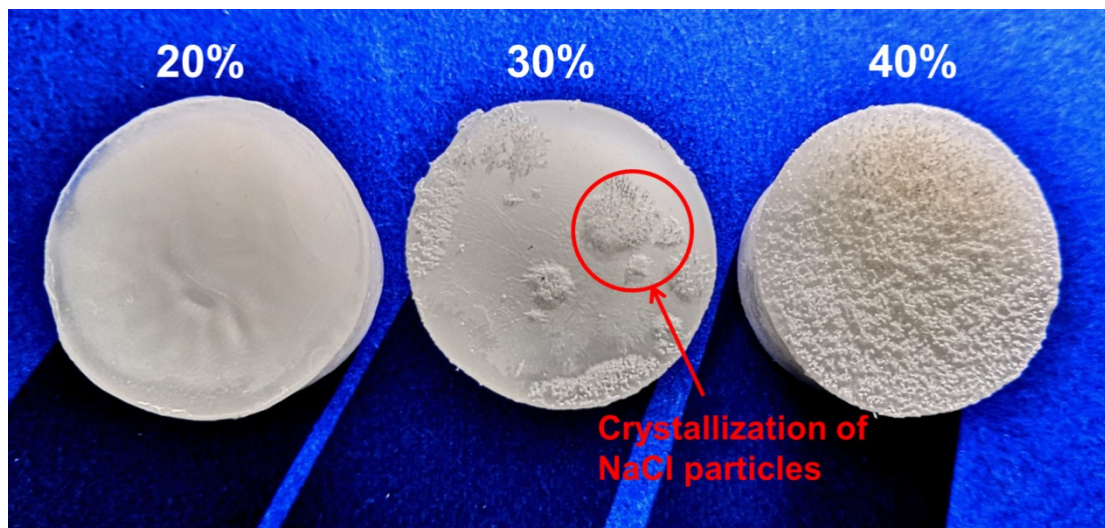


Figure S3. Image of PVA/PAM/NaCl DN hydrogels with NaCl concentration of 20%, 30% and 40%.

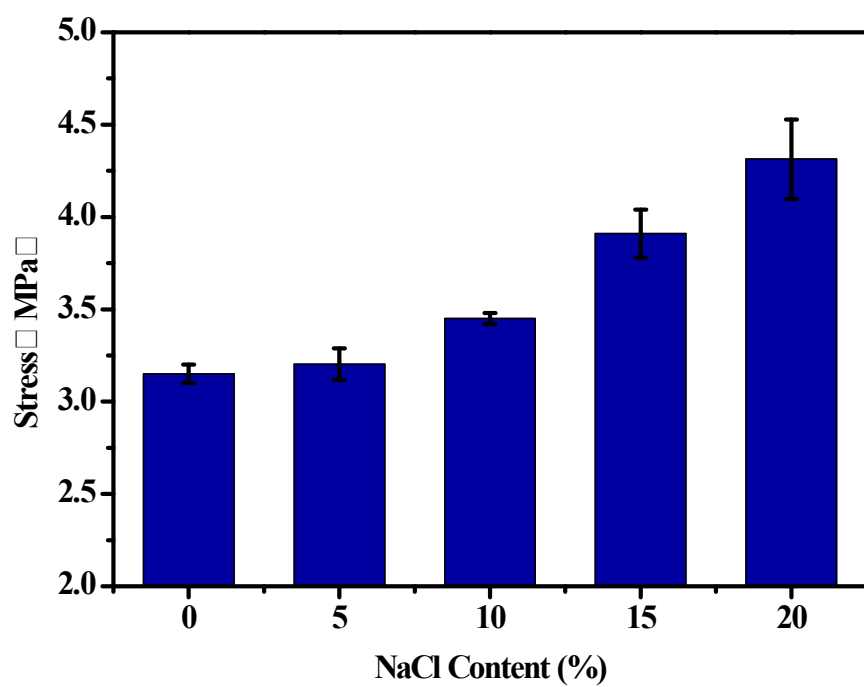


Figure S4. Compression strength of PVA/PAM DN hydrogels and PVA/PAM/NaCl DN hydrogels.

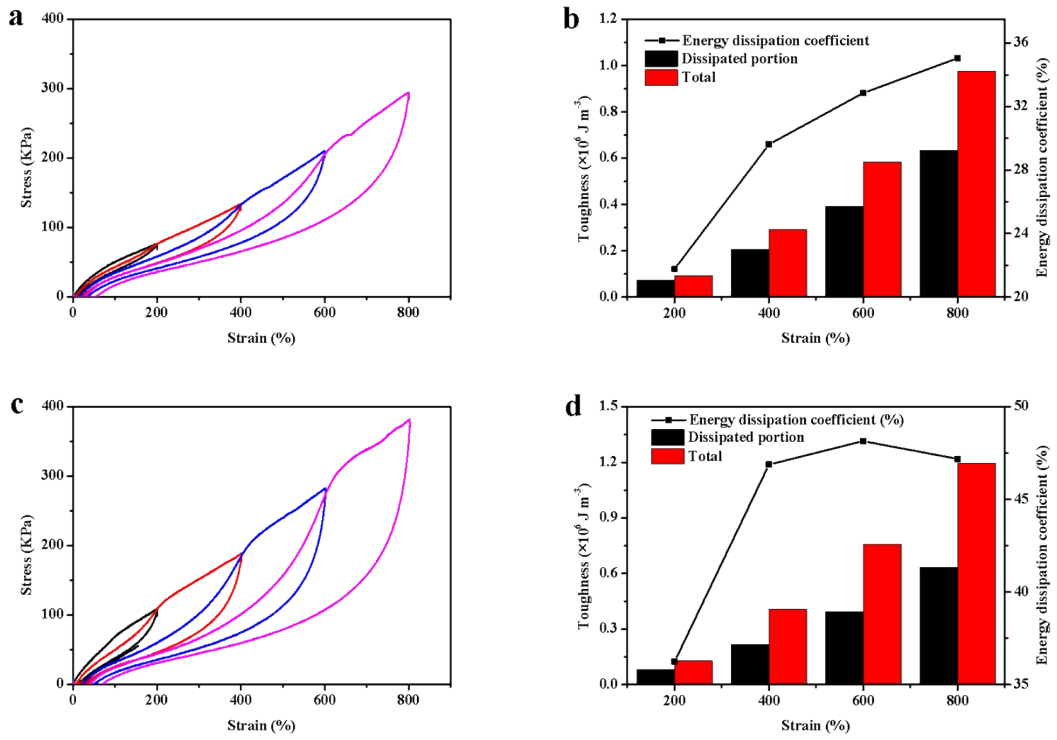


Figure S5. Loading-unloading measurement and calculated toughness and energy dissipation for a, b) PVA/PAM and c, d) PVA/PAM/NaCl-4 DN hydrogels under different strains.

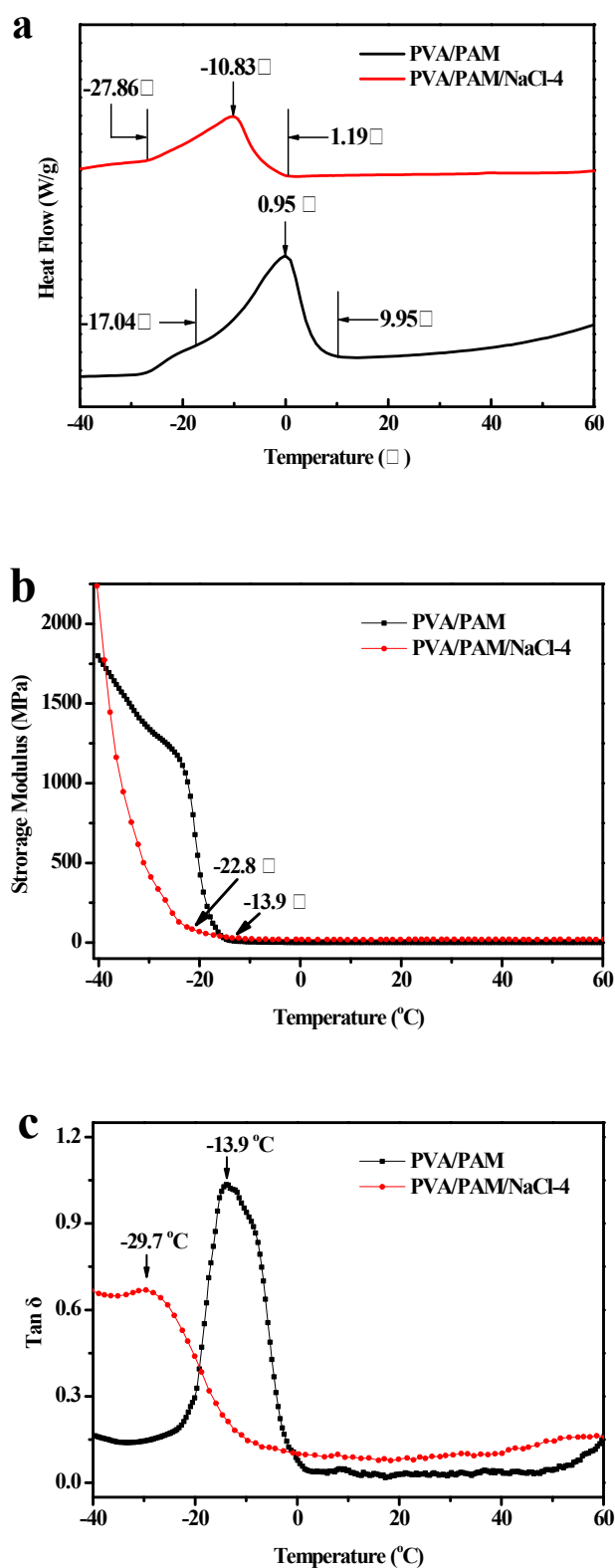


Figure S6. a) DSC curves PVA/PAM DN hydrogel and PVA/PAM/NaCl-4 DN hydrogel of and DMA curves of PVA/PAM DN hydrogel and PVA/PAM/NaCl-4 DN hydrogel: b) The storage modulus (E'), and c) The loss factor ($\tan \delta$).

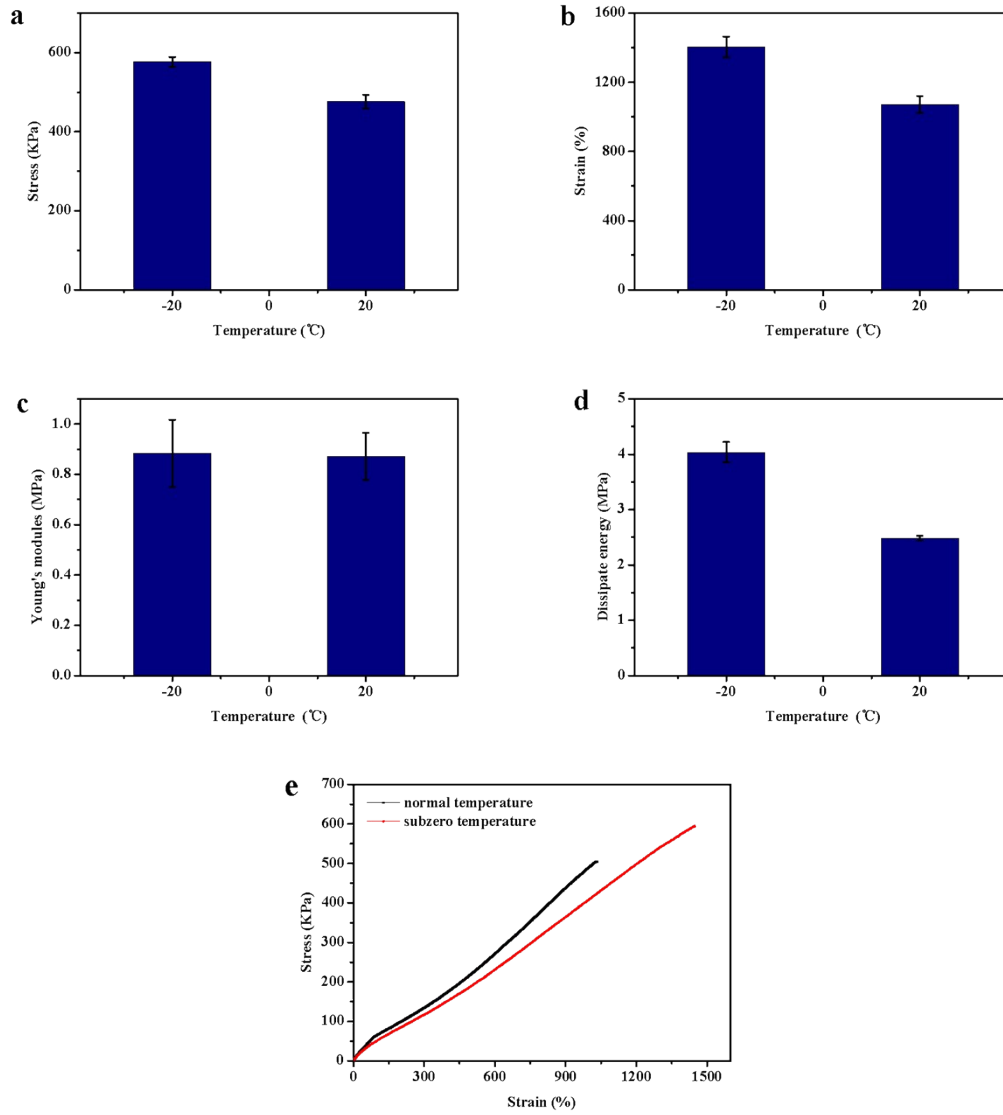


Figure S7. a) Tensile strength, b) elongation at break, c) Young's modulus, d) dissipate energy, and e) the typical tensile stress-strain curves of PVA/PAM/NaCl-4 DN hydrogels at room temperature and subzero temperature state.

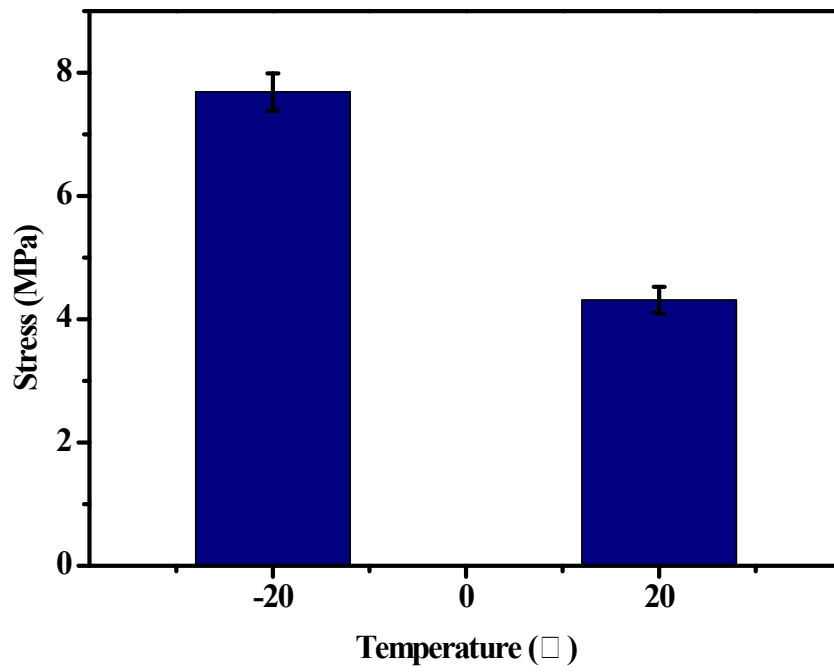


Figure S8. The compression strength of PVA/PAM/NaCl-4 at room and subzero temperature state.

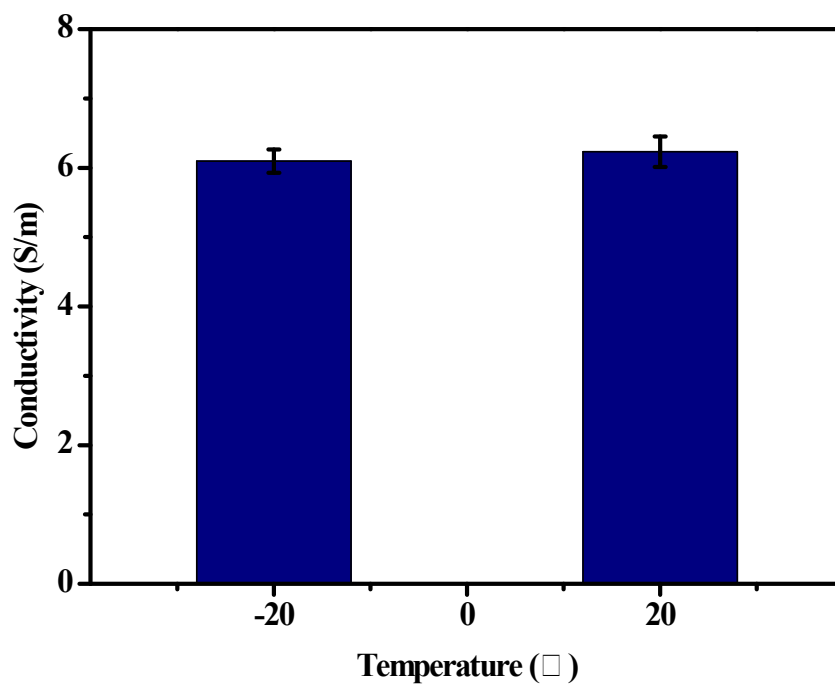


Figure S9. The conductivity values of PVA/PAM/NaCl-4 at room and subzero temperature state.

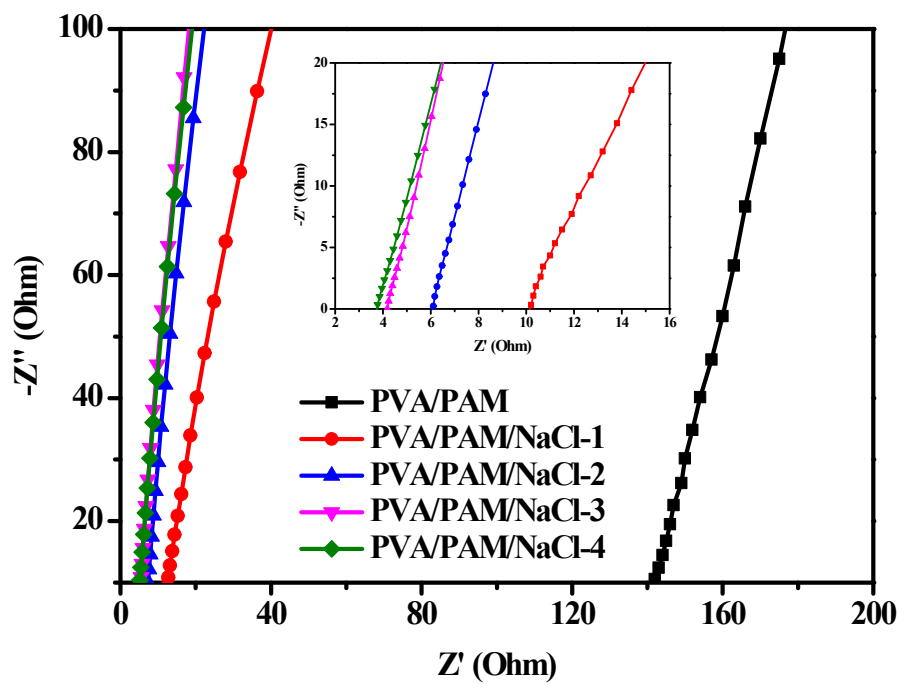


Figure S10. The Nyquist plots of PVA/PAM and PVA/PAM/NaCl DN hydrogels.

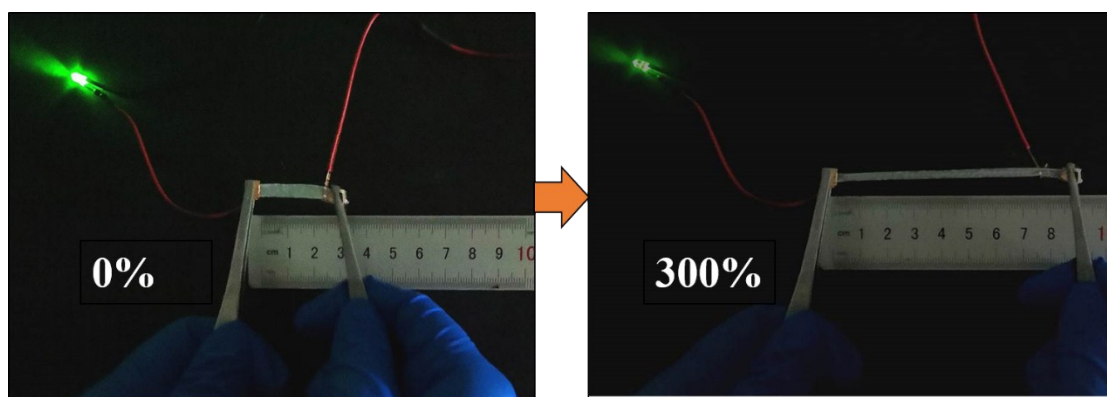


Figure S11. Photographs of the changes for LED brightness along with elongation of the hydrogel connected in the electric circuit (0% and 300%).

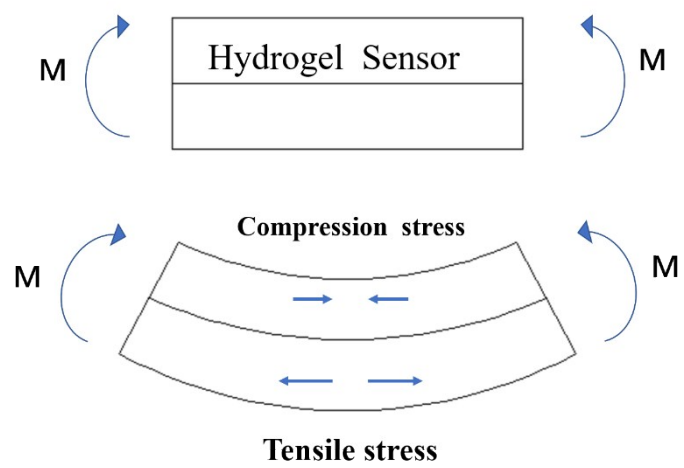


Fig S12. The illustration of the three-point bending mechanics model.

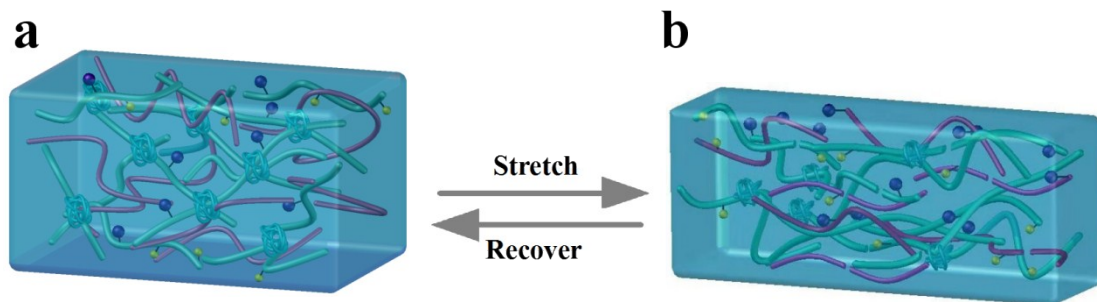
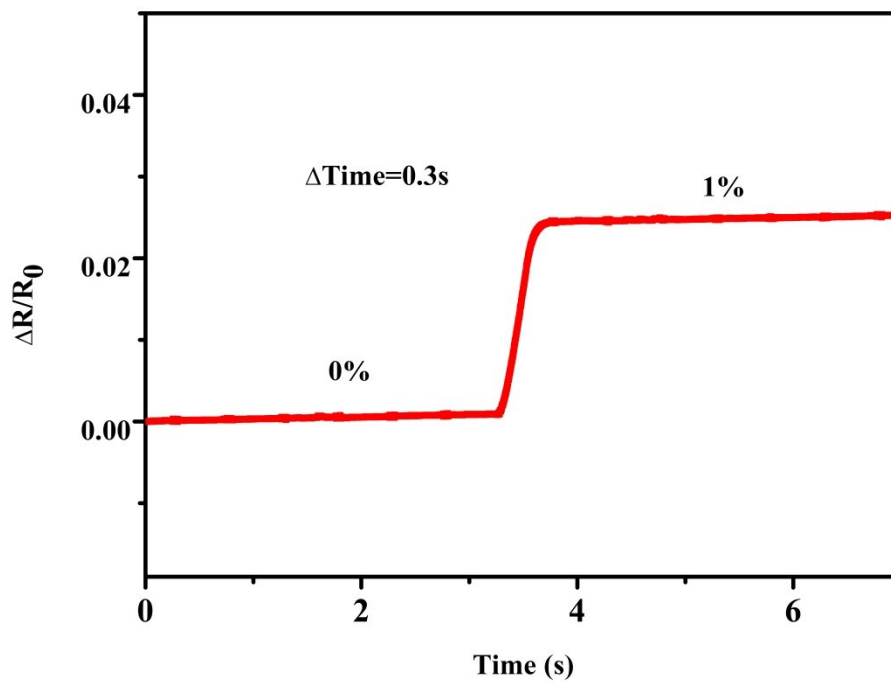


Figure S13. Schematic illustration of the conducting mechanism of the PVA/PAM/NaCl DN hydrogel electrolytes strain sensors upon stretching. The hydrogel electrolytes under a) initial state, and b) strain.

a



b

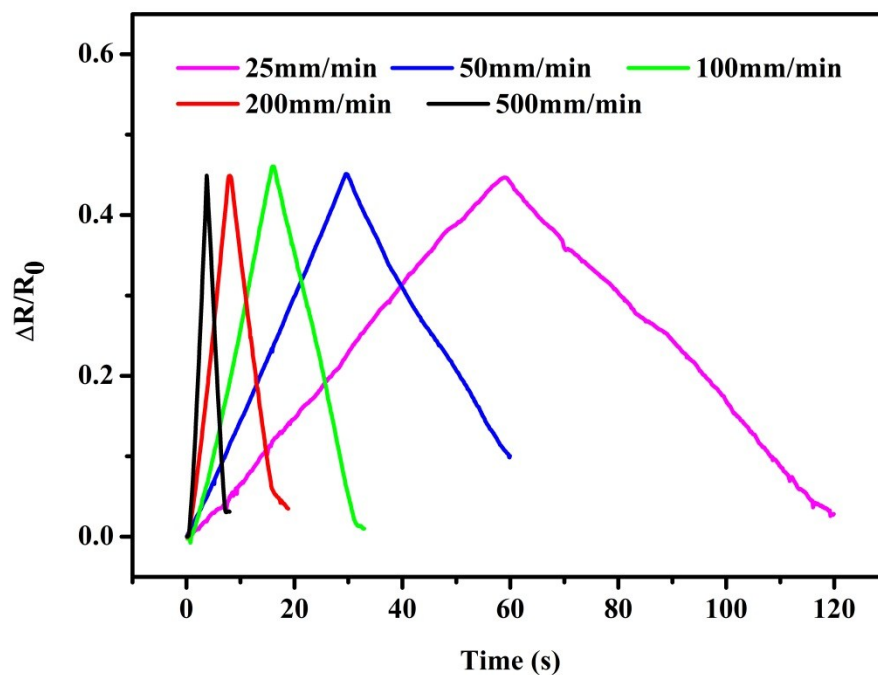


Figure S14. a) Response time of the hydrogel strain sensor, and b) The relative resistance change of sensor under cyclic stretching-releasing with a strain of 50% at stretching rates of 25–500 mm/min.

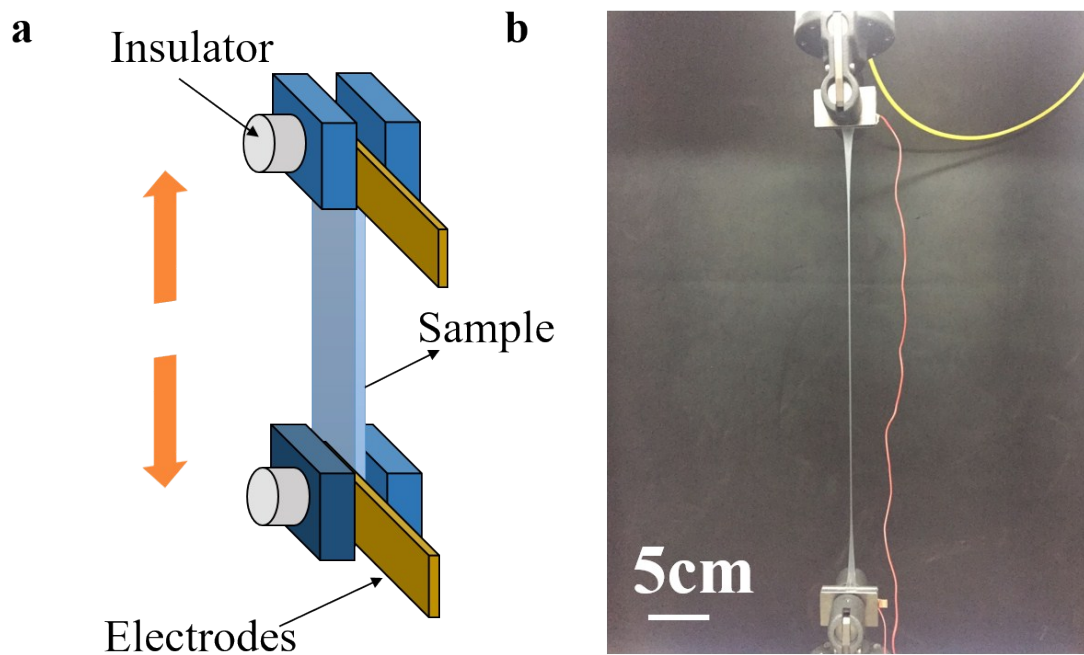


Figure S15. a) Schematic diagram, and b) experimental setup of the self-sensing test.

References

- [1] R. Tong, G. Chen, D. Pan, H. Qi, R. a. Li, J. Tian, F. Lu and M. He, *Biomacromolecules* 2019, **20**, 2096.
- [2] J. Chen, Q. Peng, T. Thundat and H. Zeng, *Chem. Mater.* 2019, **31**, 4553.
- [3] H. Liao, X. Guo, P. Wan and G. Yu, *Adv. Funct. Mater.* 2019, **29**, 1904507.
- [4] Y. Zhou, C. Wan, Y. Yang, H. Yang, S. Wang, Z. Dai, K. Ji, H. Jiang, X. Chen and Y. Long, *Adv. Funct. Mater.* 2019, **29**, 1806220.
- [5] L. Wang, G. Gao, Y. Zhou, T. Xu, J. Chen, R. Wang, R. Zhang and J. Fu, *ACS Appl. Mater. Interfaces* 2019, **11**, 3506.
- [6] Z. Wang, J. Chen, L. Wang, G. Gao, Y. Zhou, R. Wang, T. Xu, J. Yin and J. Fu, *J. Mater. Chem. B* 2019, **7**, 24.
- [7] Z. Wang, J. Chen, Y. Cong, H. Zhang, T. Xu, L. Nie and J. Fu, *Chem. Mater.* 2018, **30**, 8062.
- [8] G. Cai, J. Wang, K. Qian, J. Chen, S. Li and P. S. Lee, *Adv. Sci.* 2017, **4**, 1600190.
- [9] X. Jing, H. Y. Mi, Y. J. Lin, E. Enriquez, X. F. Peng and L. S. Turng, *ACS Appl. Mater. Interfaces* 2018, **10**, 20897.
- [10] L. M. Zhang, Y. He, S. Cheng, H. Sheng, K. Dai, W. J. Zheng, M. X. Wang, Z. S. Chen, Y. M. Chen and Z. Suo, *Small* 2019, **15**, 1.